Characteristics of Resistance Spot Welding using Annular Recess Electrodes

Article *in* Journal of Advanced Joining Processes · October 2020

DOI: 10.1016/j.jajp.2020.100035

CITATIONS
3

READS
399

3 authors:

Catherine Wandera
Kyambogo University
11 PUBLICATIONS **295** CITATIONS
SEE PROFILE

Apora James
Kyambogo University
1 PUBLICATION **3** CITATIONS
SEE PROFILE

Titus .B. Watmon
18 PUBLICATIONS **34** CITATIONS
SEE PROFILE

Journal of Advanced Joining Processes 2 (2020) 100035

Contents lists available at ScienceDirect

Journal of Advanced Joining Processes

journal homepage: www.elsevier.com/locate/jajp

Characteristics of resistance spot welding using annular recess electrodes

Titus Bitek Watmon*, Catherine Wandera, James Apora

Department of Mechanical & Production Engineering, Kyambogo University, P.O. Box 1, Kyambogo, Uganda

ARTICLE INFO

Keywords:
Resistance spot welding
Annular recess electrode
Conventional solid electrode
Welding current
Nugget diameter
Weld-integrity

ABSTRACT

Resistance spot welding is widely used in manufacturing industries, such as automobile structural body manufacture, rail vehicle construction, electronics manufacture, battery manufacture, etc. Resistance spot weld integrity is of paramount importance in the manufacturing industry, especially in automotive body joining to ensure that the automobile bodies can withstand the stress levels that the vehicle is subjected in operation. A number of factors - including electrode geometry, electrode force, welding current and welding time - influence the quality of the resistance spot weld. The electrode material that ensures electrical conductivity and compressive strength and electrode geometry defined by the electrode tip profile, shape, size are important factors in resistance spot welding. This paper discusses the comparative performance of resistance spot welding electrodes with annular recess design and the conventional solid design in welding of a 1 mm thick steel sheet used in construction of automobile structural bodies. The copper-based electrodes used in this study were prepared as described in the ISO 5182:2008 Standard. The annular recess electrode was designed using SolidWorks Version 2015; a hole measuring 4 mm deep and 2.50 mm in diameter was created centrally on the electrode tip and filled with heat resistant mixture of cement and kaolin ceramics. The effects of applied electrode force, current, and weld time on weld-integrity were investigated for the two designs of resistance spot welding electrodes. Linear regression analysis of data obtained established that the weld strength and nugget diameter was higher for the annular recess electrode than the conventional solid electrode. An analysis of variance established that the observed variation of the nugget diameter with weld time was statistically significant but the variations of weld strength with applied electrode force and variation of nugget diameter with current were not statistically significant which may require further study.

Introduction

Resistance spot welding (*illustrated in Fig. 1*) is a welding technique largely employed in manufacturing applications involving joining of sheet metal, such as car body (body in white) manufacture, rail vehicle construction, electronics manufacture, battery manufacture, etc. The resistance spot welding process is performed in three sequential steps, namely placement of electrodes with an applied pressure on surface of the sheet metal workpieces to be welded, passage of a current through the electrodes and sheet metal for a finite time duration (less than 1 second) to cause localized melting of the sheet metal, and subsequently switching off the current while leaving the electrodes in place as the melted material cools to form the bond (Zhang and Senkara, 2006). The responsiveness of the automobile industry towards energy efficiency and environmental protection have led to advancements in development of lightweight automobile bodies in which the advanced high strength steels are extensively being used; dual-phase (DP) steels are a form of composite steels whose microstructure consists of martensite and ferrite. Advanced high strength steels of varying gauges, aluminum alloy, magnesium alloy and composite materials that find application in manufacture of automobile structural bodies are commonly resistance spot welded (Shome and Tumuluru, 2015; De Cooman, 2017). The most common stainless steel that is resistance spot welded is ferritic stainless steel which has a very small amount of nickel and is a cheaper substitute to austenitic stainless steels (Amuda and Mridha, 2010). The ferritic stainless steels are widely used for structural applications in the automobile and rail coaches manufacturing industries (Pouranvari et al., 2015). The advantages of using stainless steels in structural applications include improved strength, weight reduction, improved corrosion resistance, recyclability, and high energy retention capacity under impact loads (Pouranvari and Marashi, 2012). Improvements of the resistance spot welding process, that finds much use in the automobile industry, among other industries, are directed towards optimization in aspects relating to welding of high strength materials, materials with new coatings, and difficult to weld alloys such as aluminum alloys that require high currents due to their inherent combination of high thermal and electrical conductivity.

* Corresponding author.
E-mail address: twatmon@kyu.ac.ug (T.B. Watmon).

https://doi.org/10.1016/j.jajp.2020.100035
Received 3 August 2020; Received in revised form 8 October 2020; Accepted 8 October 2020

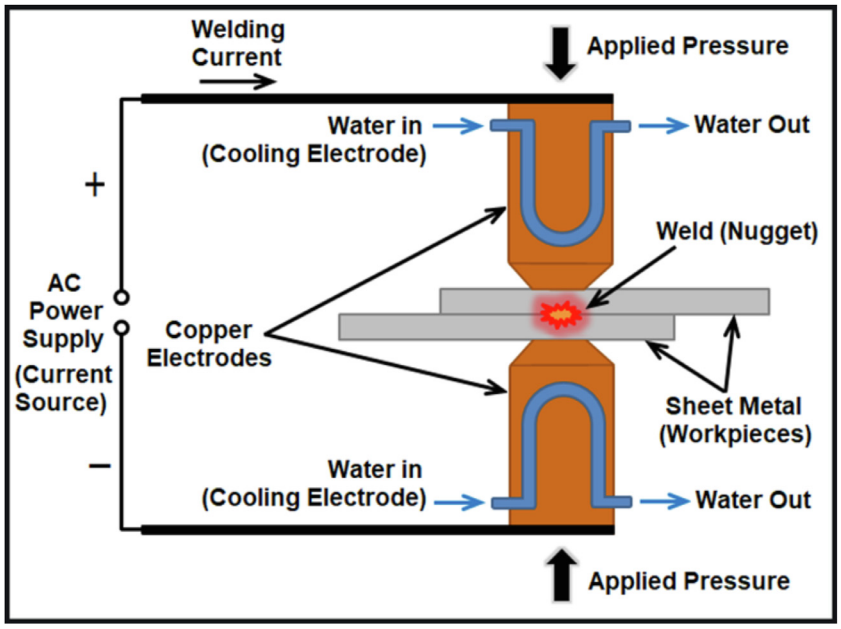

Fig. 1. Resistance spot welding technique.

Available materials indicate that resistance spot welds fail through interfacial failure involving crack propagation through the fusion zone or through pullout failure in which a weld nugget is removed from one of the joined sheets (Huin et al., 2016). According to Pouranvari and Ranjbarnoodeh (2012), resistance spot welding of dual-phase steels features problems of susceptibility to interfacial failure, expulsion where some liquid metal escapes from the nugget, formation of shrinkage voids, and high hardness in the fusion zone which influences the failure mode. Pouranvari and Ranjbarnoodeh (2012) investigated ~~of~~ the effects of welding current, welding time and electrode force on the failure mode of DP980 resistance spot welds and reported that the failure mode transformed from the interfacial mode to the pullout mode when the welding current and welding time increased at constant electrode force (Pouranvari and Ranjbarnoodeh, 2012). Ultra-high strength steels - such as Q&P980 - that are characterized by low alloy content and good mechanical properties are employed in automobile structural parts for achievement of reduced vehicle weight while ensuring a good safety performance of the vehicle. In an investigation of the microstructure of resistance spot welded joints of a 1 mm thick Q&P980 ultra high strength steel, Liu et al. (2019) identified four zones in the joint region, namely fusion zone, coarse grained heat affected zone, fine grained heat affected zone, and inter-critical heat affected zone. They reported of occurrence of recrystallization in the fusion zone and phase change in the heat affected zone; whereby lath martensite is formed in the fusion zone and coarse grained and fine grained heat affected zones while tempered martensite was formed in the inter-critical heat affected zone (Liu et al., 2019). Chabok et al. (2018) investigated the effects of single and double pulse welding on the mechanical performance of resistance spot welds in DP1000-GI steel and reported that a combination of double pulse and low welding current deteriorated the weld cross-tension strength and energy absorption capability. This was attributed to lower resistance against crack initiation and propagation due to formation of a zone of lower compressive residual stress and smaller fraction of high-angle grain boundaries in front of the pre-crack (Chabok et al., 2018). Further work by DiGiovanni et al. (2018) also compared the resistance spot welds in zinc coated and uncoated advanced high strength steel and reported that the liquid metal embrittlement (LME) during welding of coated advanced high strength steels decreased the strength in welds through a propagation of LME cracks in the periphery of the weld area until final fracture (DiGiovanni et al., 2018).

The mechanical performance of resistance spot welds in dual phase (DP) steel grades - DP600, DP780 and DP980 - was investigated by Pouranvari and Marashi (2010) who reported that the peak load and energy absorption of spot welds were governed by fusion zone size, failure mode, and strength/ductility of material at the failure zone. They observed that softening of the heat affected zone (HAZ) affected the mechanical properties of DP780 and DP980 steels which exhibit higher amounts of martensite. Softening of the HAZ results in enhanced overall ductility of the spot welds, disproportionate peak load compared to tensile strength of the base metal, and improves transition from interfacial failure to pullout failure. Moreover, the DP980 steel with higher base metal and fusion zone strength reportedly exhibited a lower tendency to interfacial failure in comparison to the lower strength DP780 steel (Pouranvari and Marashi, 2010). To address the occurrence of interfacial failure of resistance spot welds in martensitic stainless steel, Aghajani and Pouranvari (2018) modified the fusion zone microstructure by introducing a nickel interlayer to enhance the toughness of the martensitic stainless steel resistance spot welds (Aghajani and Pouranvari, 2018). Pouranvari and Marashi (2013) reviewed the process, structure and properties of resistance spot welding of automotive steels with the focus on metallurgical characteristics, hardness-microstructure correlation, failure mode and mechanical performance under various loading conditions (Pouranvari and Marashi, 2013). Pouranvari et al. (2007) used an analytical model and experiments to investigate the effects of welding current, welding time, electrode pressure and holding time on the weld nugget diameter in resistance spot welding. They reported that increasing the weld current and weld time increases the nugget diameter and weld strength up to some higher welding current and welding time after which the nugget diameter and weld strength remain constant. Additionally, the nugget diameter, weld strength and failure mode were not affected by holding time while overloading during application of force for weld nugget formation causes excessive reduction of weld nugget size, failure strength and changes in failure mode from pullout to interfacial (Pouranvari et al., 2007). Baltazar Hernandez et al. (2008) investigated the microstructure and mechanical properties of similar and dissimilar resistance spot welds in advanced high strength steels, namely a 600 MPa dual phase steel (DP600), a 780 MPa dual phase steel (DP780), and a transformation induced plasticity steel (TRIP780). They reported occurrence of interfacial failure and poor mechanical properties in DP600-DP600 welds whereas dilution of the fusion zone by DP780 in the DP600-DP780 dis-

similar welds increased the strength of the fusion zone which exhibited a martensitic microstructure. *that* softening of the heat affected zone of DP780 promoted the pullout failure mode (Baltazar Hernandez et al., 2008) which corroborates Pouranvari and Marashi (2010) finding of softening of HAZ. Pouranvari and Marashi (2012) employed a theoretical analysis and experimental study in an investigation of the correlation between metallurgical and mechanical characteristics of DP980 dual phase steel resistance spot welds with a focus on failure mode transition from interfacial mode to pullout mode. They reported that there is a minimum fusion zone size beyond which interfacial failure doesn't occur and that increasing welding current promotes pullout failure mode by increasing the fusion zone size and tempering of martensite in the sub-critical heat affected zone (HAZ). Furthermore, they reported that the fusion zone size controlled the peak load, ductility and failure energy of DP980 welds. In enhancing weld nugget corrosion resistance through improvement of fusion zone phase balance of 2304 duplex stainless steel resistance spot welds, Arabi et al. (2018) used downsloping current modification to control weld cooling rate to enable austenite formation and *in situ* post-weld short annealing to enhance formation of secondary austenite in the fusion zone (Arabi et al., 2018).

Besides the numerous studies on the metallurgical and microstructural improvements of resistance spot welding, some previous scholars (Greenwood, 1961; Holm, 1967) have also reported on the irregular heating (localized heating) in resistance spot welding which has been attributed to the non-uniform distribution of current in the electrode tip region. Greenwood (1961) (Greenwood, 1961) observed that current distribution in resistance spot welding does not flow straight across the material being welded but instead spreads into the welded sheet metal through the electrode tip circumference causing current constriction at the weld location. Later Holm (1967) noted that a current constriction occurs at the electrode face with unbalance amount of current flowing through the circumference of the electrode tip. Kaiser et al. (1982) also observed an annular molten zone around the circumference of some spot welded joints which was corroborated by Lane et al. (1987) in resistance spot welding of galvanized steel (Kaiser et al., 1982; Lane et al., 1987). Consequently, it is clear that the performance characteristics of a resistance electrode depends on the electrode geometry having a bearing on the heating condition spread over the electrode tip surface as Friedman and McClauley (1969) identified it to be one of the factors that facilitate increased rate of electrode tip deformation (Friedman and McCauley, 1969). The initial temperature patterns in resistance spot welding as observed by Greenwood (1961) indicated a maximum temperature value in a ring around the circumference of the electrode tip that resulted into an assertion that a ring weld would form if the current were high enough to produce a weld in a short time. The phenomenon of a ring weld was also corroborated by Neid (1984) through a study which involved finite element modeling of the resistance spot welding process (Neid, 1984) thus the prevalence of uniform current distribution at the outer circumference of the electrode tip illustrates the fact that current constricts around corners such as the angle between the tapered end of a truncated cone electrode and the workpiece. The electrode contact area geometry is very important in the resistance spot welding process; the electrode tip diameter should be slightly larger than the nugget diameter for good weld results to be obtained. The weld (nugget) formed will be smaller and weaker when the electrode tip diameter is smaller but also overheating occurs when the tip diameter is too large resulting in formation of voids. Meanwhile, Dulal et al. (2014) reported that conventional spot-welding tools produce joints which are stronger at the edges but weaker in the center of the nugget which presumably experiences high voltage concentrations (Dulal et al., 2014). Watanabe et al. (2016) investigated the cross-tension strength of resistance spot welds made using a concave electrode in welding of high-strength steel sheets (HSSS) and reported an improvement in joint strength of approximately 1.5 times for a welded joint made using the concave electrode compared to the conventional electrode (Watanabe et al., 2016). Furthermore, nugget diameter in resistance spot welding depends on current intensity, weld-time, electrode force and geometry. Bowers et al. (1990) studied the relationship between electrode geometry, current distribution and electrode life and reported that higher angles of electrode-workpiece interface resulted in more uniform current distribution at the electrode tip surface. And that equal current distribution at the electrode tip yielded even wear of the electrode tip, although higher angles rapidly facilitated burgeoning of the tip (Bowers et al., 1990). Using the principles of thermodynamics and heat transfer, Zhou and Cai (2014) developed a model for estimating the nugget growth process based on the heat energy delivered into the welds by the resistance spot welding and the effect of electrode force during the welding process (Zhou and Cai, 2014). The applied electrode force during the resistance spot welding process is one of the most important parameter which influences the resistance spot welding process and affects the resulting weld strength (Zhou and Cai, 2014).

Therefore, this paper presents a comparative experimental investigation of the performance of an annular recess resistance spot welding electrode and a conventional resistance spot welding electrode. The effects of welding current and electrode force on weld strength are comparatively investigated for the two cases of the conventional electrode and the annular recess electrode. High weld strengths are usually required for automobiles body fabrication so that the automobile bodies can withstand the stress the vehicle goes through on the different road terrains and conditions.

Experimentation

Description of sheet metal used

The mild steel sheet metal of gage 18 with a thickness of 1 mm was used in this experimental study based on common knowledge of materials normally used in vehicle manufacturing industries where Resistance Spot Welding (RSW) is highly practiced in the manufacture of the car body. The sample sheet metal used was extracted (salvaged) from a written off Range Rover motor vehicle and the same thickness of sheet metal was used throughout the investigation. The gauges 28–30 were not used in this study because such gauges are too thin to withstand high welding current and long weld time.

Description of electrodes used

Two types of electrodes were used in this comparative study of the performance of an annular recess electrode and the conventional solid electrode in resistance spot welding; this section provides the descriptions of the two designs of electrodes used. The two designs of spot welding electrodes were machined out of a copper rod and both designs have a 45° conical end with the electrode tip diameter of 6 mm. The depth of the cooling hole in both the lower and upper electrodes were machined to the Resistance Spot Welding (RSW) machine manufacturer specifications. Copper was used as the electrode material according to the ISO 5182:2015 standard which specifies materials for resistance welding electrodes (5).

The annular recess resistance spot welding electrode

A novel resistance spot welding electrode featuring an annular recess region in the contact area between the electrode and workpiece was designed in this study using SolidWorks version 2015. The specified annular recess electrode design features include a 16 mm diameter copper rod with a 45° taper/conical region towards the electrode face tip (*i.e. electrode-workpiece contact region*) of 6 mm diameter on which there is a 2.5 mm annular recess hole of 4 mm depth at the center of the electrode face tip as shown in Fig. 2. The associated mass properties of novel annular recess electrode were also generated to provide an in-depth description on the physical properties for the electrode design specification.

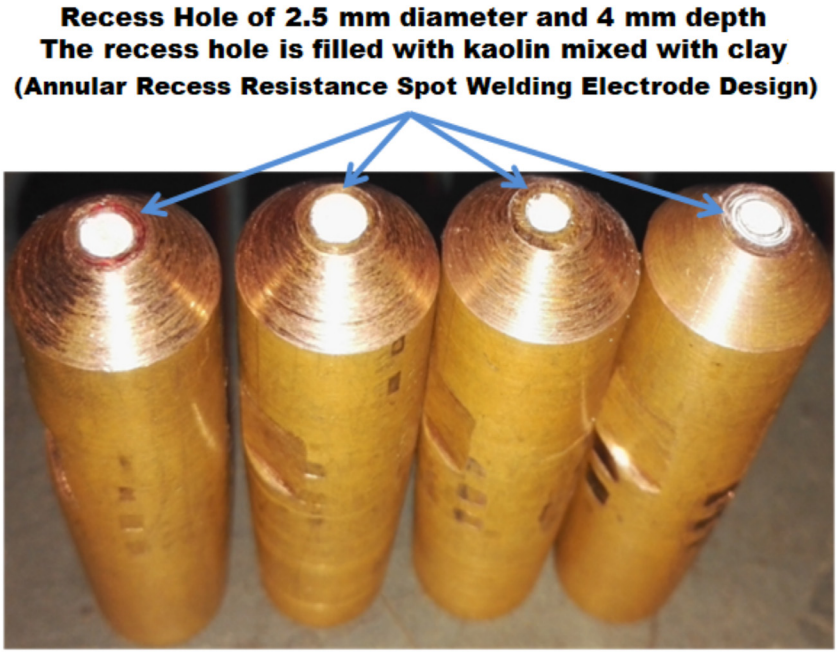

Fig. 2. Annular recess spot welding electrodes used in the study.

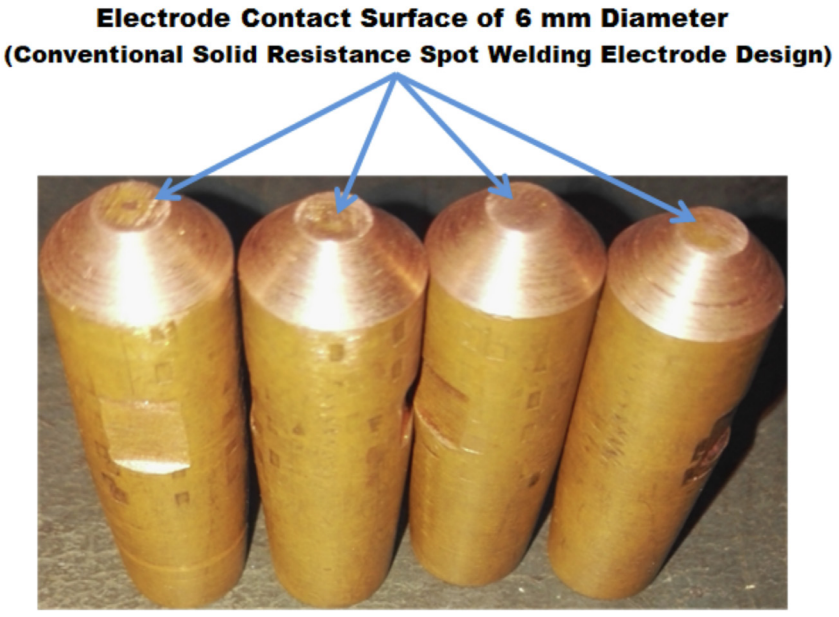

Fig. 3. Conventional solid spot welding electrodes used in the study.

In the manufacture of the annular recess electrode, a piece of copper rod of diameter 16 mm was set on a three-jaw lathe chuck and the front end was contour-turned to 6 mm diameter at the face tip followed by centrally drilling an annular recess hole of 2.5 mm diameter on the 6 mm diameter face tip. The recess hole in the novel annular recess electrode design was filled with an insulating material; a mixture of ceramic kaolin (porcelain), clay and Portland cement was used as the insulating material which can withstand temperature upto 3272° F. The clay Kaolin mixture was flush finished on the electrode to create the annular contact surface.

The conventional solid resistance spot welding electrode

The conventional solid resistance spot welding electrode used in this study was a 16 mm diameter copper rod with a 45° taper/conical region towards the electrode face tip (*i.e. electrode-workpiece contact region*) of 6 mm diameter as shown in Fig. 3.

Description of experimental procedure and equipment used

Properties of the steel sheet workpiece

The chemical composition of the steel sheet metal workpiece used in this study was determined through a chemical analysis using an Atomic Emission Spectrometry. A specimen of the steel sheet measuring 40 mm by 40 mm was prepared for chemical composition analysis using an atomic emission spark spectrometry machine and the determined chemical composition of the steel sheet is shown in Table 1 on the next page. The chemical composition of the steel sheet was 0.03% wt C, 0.21% wt Mn, and 99.5% wt Fe which indicates that the sheet metal was a ferritic steel alloy with ferromagnetic properties. Additionally, the physical properties of the steel sheet workpiece material were determined by subjecting the steel sheet to destructive tests, namely tensile and hardness tests using the tensile testing machine (*Denison Model T42-B4*) and hardness testing machine (*HOYTOM Model Super Rockwell-Duplex 713-SR,*

Table 1
Chemical composition of the steel sheet workpiece material (wt %).

C	Si	Mn	P	S	Cr	Mo	Ni
0.0305	0.0110	0.213	0.0114	0.0111	0.0460	0.0010	0.0015
Al	**Co**	**Cu**	**Nb**	**Ti**	**V**	**W**	**Pb**
0.0388	0.0033	0.0472	0.0019	0.0002	0.0052	0.0050	0.0018
Sn	**AS**	**Zr**	**Bi**	**Ca**	**Ce**	**Sb**	**Se**
0.0032	0.0076	0.0018	0.0010	0.0001	0.0060	0.0012	0.0035
Te	**Ta**	**B**	**Zn**	**La**	**N**	**Fe**	**CEQ**
0.0017	0.0070	0.0013	0.0029	0.0003	0.0024	**99.5**	0.0797

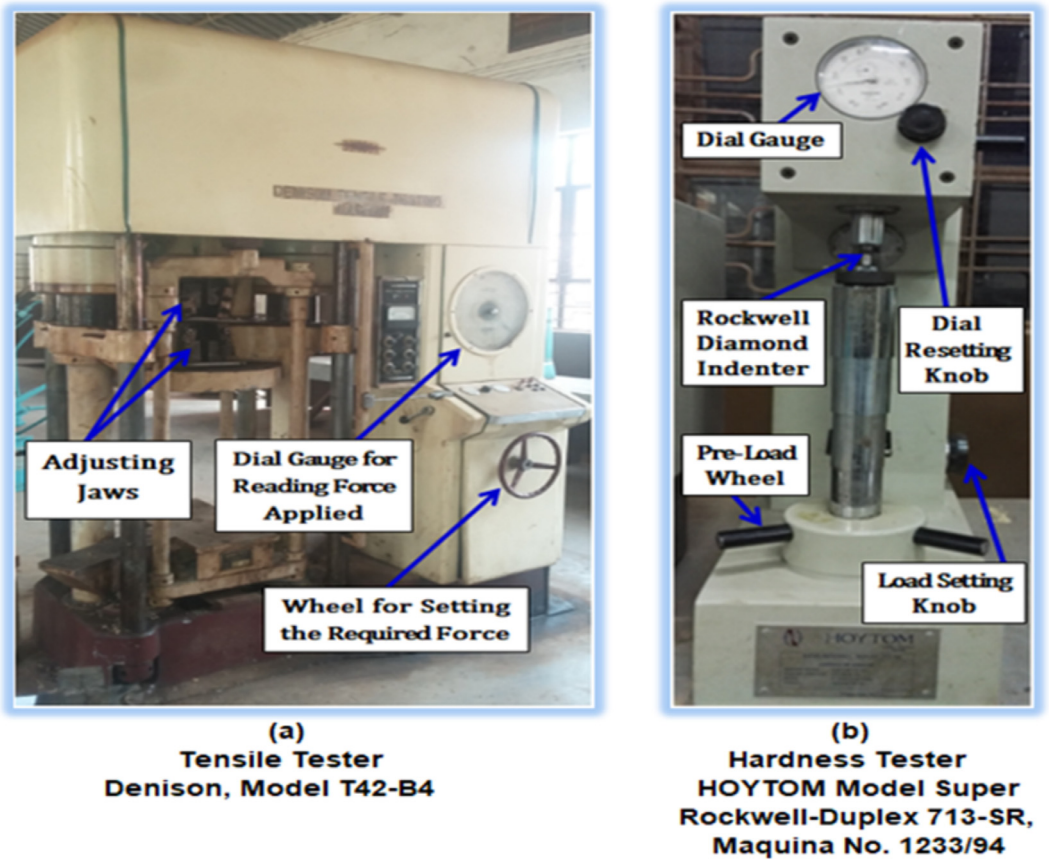

Fig. 4. Tensile testing and hardness testing equipment used.

Maquina No. 1233/94) shown in Fig. 4a and b available at Kyambogo University Materials Testing Laboratory. Specimens of the steel sheet metal of 1 mm thickness were prepared into a 50 mm by 175 mm sizes; the ends of the prepared specimen were supported alternately on the jaws of the tensile testing machine using spacers. Each of the prepared specimens was subjected to a maximum peak load in order to determine the maximum elongation and ultimate tensile strength. Additionally, the hardness of the steel sheet workpiece was determined using the hardness test carried out on a specimen measuring 50 mm by 50 mm. Five random hardness readings were taken at five different random points on the specimen surface and the average value was recorded. The physical properties of the steel sheet workpiece material used in this study, namely ultimate tensile strength (UTS), percentage elongation and hardness are shown in Table 2 below.

Table 2
Mechanical properties of the 1 mm steel sheet workpiece material.

Ultimate tensile strength (KN)	Percentage elongation (%)	Hardness
2400	32	HRC 88.3

Purity of the resistance spot welding electrodes

Spark emission spectrometry was used to establish the purity of the resistance spot welding electrodes used in this study which characterizes their thermo conductivity. Specimens were prepared from the copper rod used for manufacture of both the annular and conventional resistance spot welding electrodes and subjected to the spark emission spectrometry tests. The chemical composition of the copper rod used for manufacture of the copper electrodes used in this study is shown in Table 3. The chemical composition of the electrode material used shows that the electrodes had over 80 wt% copper and most of the alloy elements are less than 1% which indicates that the electrodes are a copper alloy with significant purity, thus; it is highly thermo-conductive.

Resistance spot welding experiments

The BS EN ISO 14,271:2017 standard for resistance spot welding and seam welding was strictly followed during the resistance spot welding experiments (5). In accordance with the BS EN ISO 14,271:2017 stan-

Table 3
Chemical composition of the copper rod used for electrodes (wt %).

C	Si	Mn	P	S	Cr	Mo	Ni
0.0458	0.0122	0.0141	0.0166	0.0099	0.0052	0.0890	0.0520
Al	**Co**	**Cu**	**Nb**	**Ti**	**V**	**W**	**Pb**
0.0021	0.0742	>8.0	0.0408	0.0333	0.0047	0.0617	0.0261
Sn	**Mg**	**As**	**Zr**	**Bi**	**Ca**	**Ce**	**Sb**
0.0097	0.0069	0.0110	0.0033	0.0040	0.0007	0.0131	0.151
Se	**Te**	**Ta**	**B**	**Zn**	**La**	**N**	
0.0010	0.0800	>0.760	0.0015	>0.045	0.0043	0.302	

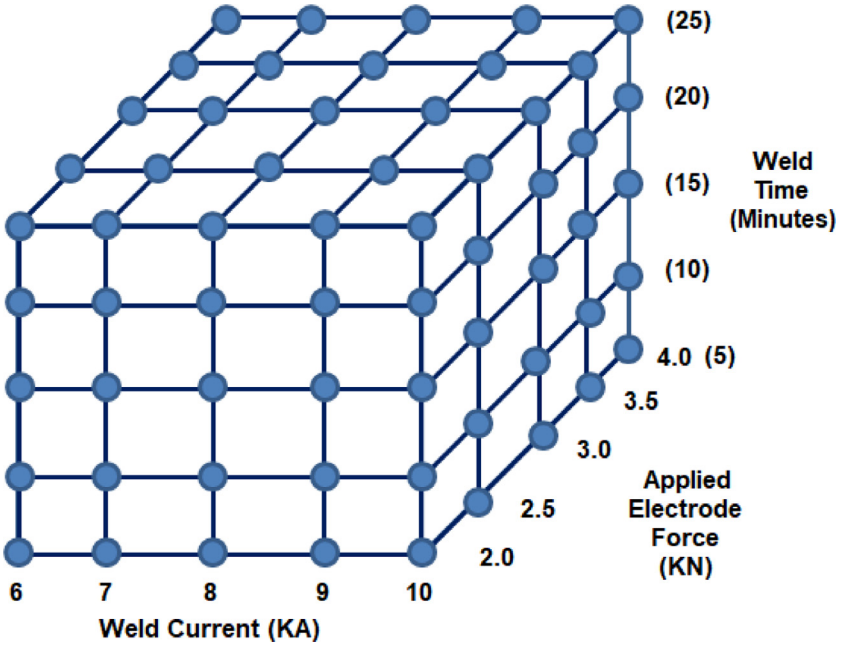

Fig. 5. Design of the resistance spot welding experiments.

dard, the following ranges of resistance spot welding parameters were used in the experiments; current (6 to 10 KA), weld time (5 to 25 min), and applied force (2 to 4 KN); the details of the experimental design are presented in Fig. 5. The resistance spot welding experiments were carried out with both the novel annular recess resistance spot welding electrode and the conventional resistance spot welding electrode which has a complete contact surface. Two annular recessed electrodes were mounted on both the upper and lower jaws of the Resistance Spot Welding machine. For all these resistance spot welding investigations, the annular recess electrodes used had an electrode tip with an outer diameter of 6.0 mm and a central recessed hole of 2.5 mm diameter which was 4 mm deep; and the conventional electrode used featured a solid electrode tip of 6 mm diameter.

Evaluation of the weld quality

The destructive tests (DT) that were carried out to test the quality of the welded joints followed the BS EN ISO 9018:2015 standard (2015) destructive tensile tests on welds in sheet metals (5) and the BS EN ISO 10,447:2015 standard (2015) for peel and chisel test (5). In analyzing the test results, this study used linear regressions analysis based on the formula in Eq. (1) to establish the relationships between the independent variables (electrode force, weld current, and weld time) and the dependent variables (maximum tensile load and nugget diameter). Additionally, the significance of the observations indicated by the results was evaluated using an analysis of variance (ANOVA).

$$\hat{Y} = aX + b \quad (1)$$

Where

a - Slope of regression
$\hat{Y}$ - Predicted value of Y
X - Independent variable (predictor variable)
b - Intercept (value of Y when $X = 0$)

Results and discussion

Effect of electrode geometry on weld strength

The effect of electrode geometry on weld strength was investigated by determining the variation of the maximum tensile load on the welded joints with applied electrode force for both the conventional solid electrode and the annular recess electrode as shown in Fig. 6. It was generally observed that the maximum tensile strength of the welded joint was higher when welding was performed using the annular recess electrode than when the conventional (solid) electrode was used; however, the observed variation in maximum tensile load with electrode geometry was not linear indicating that there might be other additional influencing variables. Nevertheless, the linear regression analysis providing the correlation of weld strength and applied electrode force indicates a strong positive correlation for the annular recess electrode with Pearson coefficient, R of 0.8 and a negative correlation for the conventional solid electrode having a negative Pearson coefficient, R of −0.6. This means that the use of the annular recess electrode in resistance spot welding improved the weld joint strength by almost 1.5 times the performance of the conventional solid electrode. This result agrees with the findings of Watanabe et al. (2016) who used a concave electrode in welding of high-strength steel sheets (HSSS) and reported a larger maximum tensile load of 8 KN for a welded joint of 6.5 mm nugget diameter made using the concave electrode compared to the maximum tensile load of 5.5 KN obtained with a conventional electrode indicating an improvement in joint strength of approximately 1.5 times (Watanabe et al., 2016). However, an analysis of variance shown in Table 4 established that the

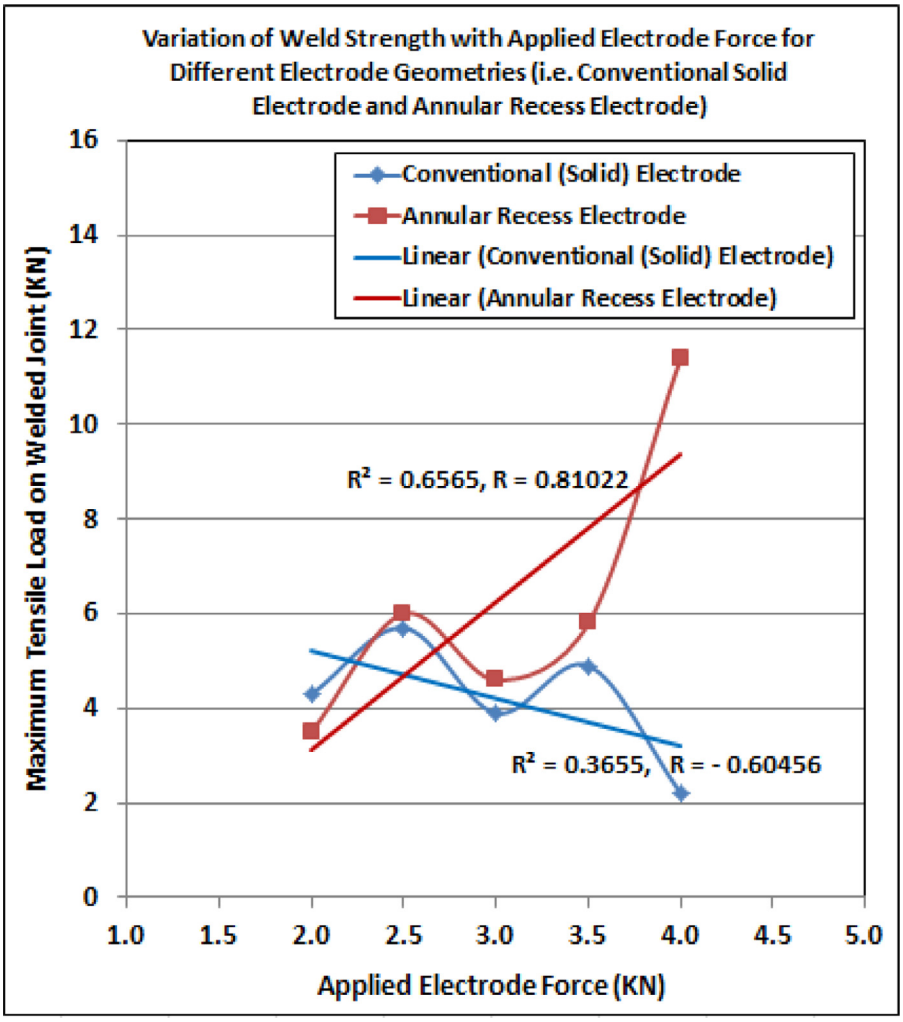

Fig. 6. Weld strength vs. applied electrode force for different electrode geometries.

Table 4
Effect of electrode force on weld strength for different electrode geometry.

ANOVA: Two-factor without replication						
Source of variation	*SS*	*df*	*MS*	*F*	*P-value*	*F crit*
Applied electrode force	11.186	4	2.797	0.342	0.838	6.388
Electrode geometry	10.609	1	10.609	1.297	0.318	7.709
Error	32.726	4	8.182			
Total	54.521	9				

variation of weld strength with electrode force for the two electrode geometries used (namely annular recess electrode and conventional solid electrode) was not statistically significant. This could be pointing to a possibility that the observed variation could be resulting from multiple effects and needs to be investigated further.

Effect of electrode geometry on nugget diameter

The effect of electrode geometry on nugget diameter was investigated by determining the variation of nugget diameter with current and also the variation of nugget diameter with weld time for both the conventional solid electrode and the annular recess electrode. Fig. 7 shows a clear correlation between the amount of current spent in the weld and the resulting nugget diameter for both the annular recess electrode and the conventional solid electrode. The annular recess electrode generally produced a larger nugget diameter in comparison to the conventional solid electrode although the observed variation was not linear indicating that there might be other additional influencing variables. The linear regression analysis shows that the correlation between the amount of current and nugget diameter was higher for the annular recess electrode with a Pearson coefficient, R of 0.58 and was lower for the conventional solid electrode which had a Pearson coefficient, R of 0.48. This finding agrees with the model of Zhou and Cai (2014) for estimating the nugget growth process based on the heat energy delivered into the welds by the resistance spot welding and the effect of electrode force during the welding process (Zhou and Cai, 2014). Our finding is also consistent with the findings of Watanabe et al. (2016) who observed that 'nuggets with a diameter of approximately 6.5 mm were formed with a large current of 8 kA which could not be set when using the conventional electrode (Watanabe et al., 2016). An analysis of variance shown in Table 5 indicates that the variation of nugget diameter with current for the annular recess electrode and conventional solid electrode was not statistically significant; therefore, the observed variation could be resulting from various influencing factors which couldn't be established

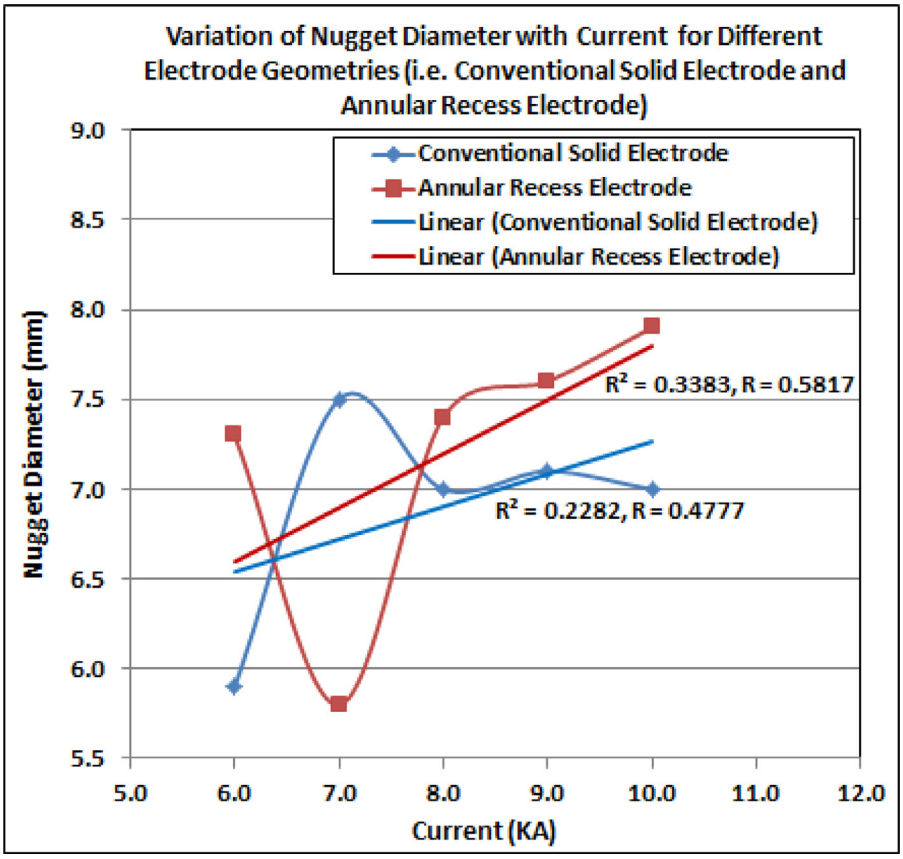

Fig. 7. Nugget diameter vs. current for different electrode geometries.

Table 5
Effect of current on nugget diameter for different electrode geometry.

ANOVA: Two-factor without replication						
Source of variation	*SS*	*df*	*MS*	*F*	*P-value*	*F crit*
Current	1.270	4	0.318	0.452	0.770	6.388
Electrode geometry	0.225	1	0.225	0.320	0.602	7.709
Error	2.810	4	0.703			
Total	4.305	9				

Table 6
Effect of weld time on nugget diameter for different electrode geometries.

ANOVA: Two-factor without replication						
Source of variation	*SS*	*df*	*MS*	*F*	*P-value*	*F crit*
Weld time	0.296	4	0.074	1.609	0.328	6.388
Electrode geometry	1.521	1	1.521	33.065	0.005	7.709
Error	0.184	4	0.046			
Total	2.001	9				

precisely within the scope of the investigation in this study. According to Bowers et al. (1990), the electrode-workpiece interface angles approaching 90° facilitate more equal current distribution at the electrode tip which implies that electrode geometry affects tool life and wear as result of its influence on the local current distribution (Bowers et al., 1990). A worn out electrode geometry tends to shift the position of the welding hemisphere. In the investigations undertaken in this study, the electrodes showed signs of gradual wear which resulted into weld joints with weak fusion and asymmetrical nugget formation thereby, generating poor quality welds. Therefore, it was necessary to constantly inspect the electrode life and appropriate action taken to restore the electrode condition by regrinding.

Effect of weld time on nugget diameter for different electrode geometries

In investigating the effect of weld time on nugget diameter, the weld time was taken at an interval of 5 min cycle. Fig. 8 shows a correlation between the weld time and the resulting nugget diameter for both the conventional solid electrode and the annular recess electrode; the nugget diameter was generally higher for welds made using the annular recess electrode than for welds made using the conventional solid electrode. It can be seen from Fig. 8 that the annular recess electrode consistently gave bigger nugget diameter in comparison to the conventional solid electrode. The nugget diameter for the weld joints formed using the annular recess electrode varied from 5.8 mm to 8.4 mm compared to 5.9 mm – 7.8 mm nugget diameter for weld joints formed using the conventional electrode. The annular recess electrode gave a nugget diameter of 7.9 and the conventional tool generated a diameter of 7.3 at a cycle time of 5 min; and a nugget diameter was 8.1 mm for the annular recess electrode and 7.7 mm for conventional solid electrode at cycle time of 25 min.

The linear regression analysis shows that the correlation between the nugget diameter and weld time was higher for the annular recess electrode with a Pearson coefficient, R of 0.69 than with the conventional solid electrode which had a Pearson coefficient, R of 0.48. Table 6 shows the results of an analysis of variation of nugget diameter with weld time for the annular recess electrode and conventional solid electrode which indicates that the variation of nugget diameter with electrode geometry is statistically significant. The annular recess configuration used for spot welding process offered greater surface area with low aspect ratio resulting in faster and controlled cooling of the molten weld layer which then fuses towards the center of the weld joint and expands outwards forming a larger nugget diameter.

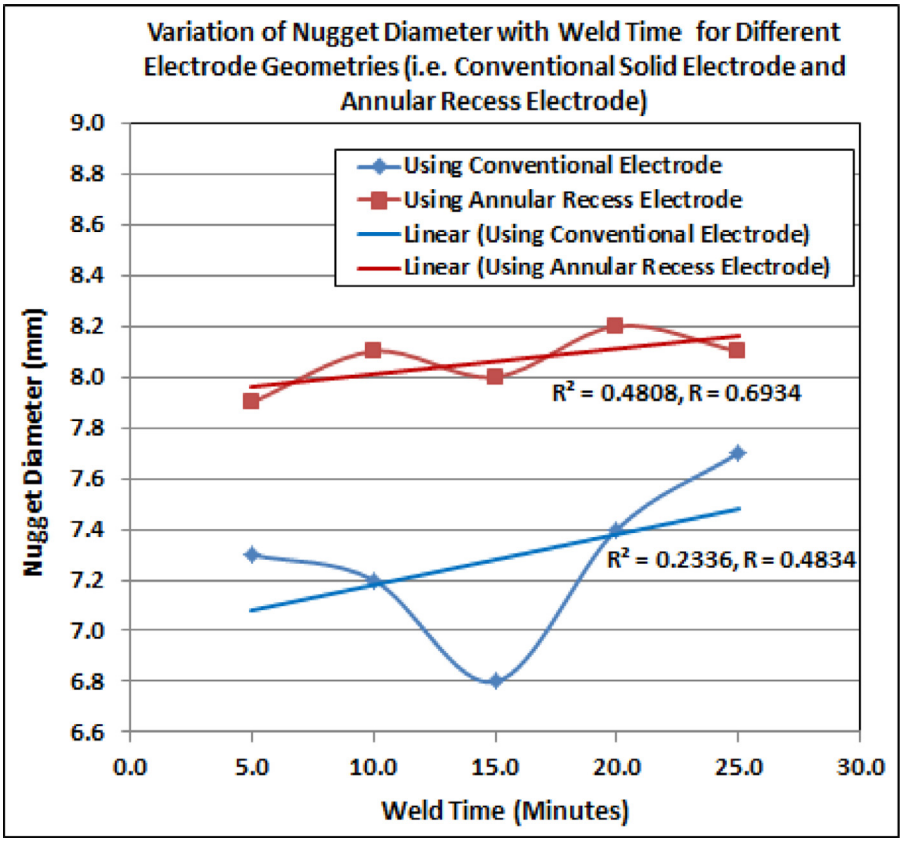

Fig. 8. Nugget diameter vs. weld time for different electrode geometries.

Conclusion

The weld integrity of resistance spot welds is of paramount importance in the manufacturing industry, especially in automotive body joining, to ensure reliable functionality of the manufactured products. This study investigated the performance of the annular recess electrode in comparison to the conventional solid electrode in resistance spot welding of a steel sheet metal. The performance characteristics of the two electrode designs were evaluated by examining the variation of weld strength with applied electrode force and the variation of nugget diameter with current and weld time. It was established that the annular recess electrode produced higher weld strength and larger nugget diameters compared to the conventional electrode. A statistical analysis of the effect of weld time on nugget diameter was statistically significant for both the annular recess electrode and conventional electrode. However, the effects of applied electrode force on weld strength and effects of current on nugget diameter were not statistically significant within the scope of the investigation in this study. This might point to other variables influencing the performance of the annular recess electrode in resistance spot welding and could constitute a focus of a future study in this area.

Declaration of Competing Interest

We have no conflict of interest to declare.

References

Aghajani, H., Pouranvari, M., 2018. A pathway to produce strong and tough martensitic stainless steels resistance spot welds. Sci. Technol. Weld. Join. doi:10.1080/13621718.2018.1483065.

Amuda, M., Mridha, S., 2010. Grain refinement in ferritis stainless-steel welds: the journey so far. Adv. Mater. Res. 83-86, 1165–1172.

Arabi, S., Pouranvari, M., Movahedi, M., 2018. Pathways to improve the austenite-ferrite phase balance during resistance spot welding of duplex steels. Sci. Technol. Weld. Join. doi:10.1080/13621718.2018.1468949.

BS EN ISO 9018: 2015 Standard. (2015). Standard for destructive tests on welds in metallic materials.

BS EN ISO 10447: 2006 Standard. (2015). Standard for resistance welding - peel and chisel testing of resistance spot and projection welds.

Baltazar Hernandez, V., Kuntz, M., Khan, M., Zhou, Y., 2008. Influence of microstructure and weld size on the mechanical behaviour of dissimilar AHSS resistance spot welds. Sci. Technol. Weld. Join. 13 (8), 769–776.

Bowers, R., Sorensen, C., Eagar, T., 1990. Electrode geometry in resistance spot welding. Weld. J. 45-s–51-s.

Chabok, A., Van der Aa, E., Basu, I., De Hosson, J., Pei, Y., 2018. Effect of pulse scheme on the microstructural evolution, residual stress state and mechanical performance of resistance spot welded DP1000-GI steel. Sci. Technol. Weld. Join. 23 (8), 649–658. doi:10.1080/13621718.2018.1452875.

De Cooman, B., 2017. High Mn TWIP steel and medium Mn steel. In: Automotive Steels: Design, Metallurgy, Processing and Applications. Woodhead Publishing, pp. 317–385.

DiGiovanni, C., Biro, E., Zhou, N., 2018. Impact of liquid metal embrittlement cracks on resistance spot weld static strength. Sci. Technol. Weld. Join. doi:10.1080/13621718.2018.1518363.

Dulal, C.S., et al., 2014. Heat-affected zone liquation on resistance spot welded TWIP steels. Mater. Charact. 93, 40–51.

Friedman, L., McCauley, R., 1969. Influence of metallurgical characteristics on resistance welding of galvanized steel. Weld. J. 48 (10), 454–462.

Greenwood, S., 1961. Temperatures in spot welding. Br. Weld. J. 8 (6), 316–322.

Holm, R., 1967. Electrical Contact: Theory and Application. Springer Verlag, New York, pp. 9–18.

Huin, T., Dancette, S., Fabrègue, D., Dupuy, T., 2016. Investigation of the failure of advanced high strength steels heteregoneous welds. Met. Basel 6. doi:10.3390/met6050111. www.mdpi.com/journal/metals.

ISO 5182: 2016 Standard. (2016). Resistance welding. Materials for electrodes and ancillary equipment which are used for carrying current and transmitting force to the workpiece.

ISO 14271: 2017: Standard. (2017). Standard for resistance welding, welded joints, welding, Vickers hardness measurement (low force and micro harness) of resistance spot, projection and seam welding.

Kaiser, C., Dunn, G., Eagar, T., 1982. The effect of electrical resistance on nugget formation during spot welding. Weld. J. 62 (6), 164–174.

Lane, C., Sorensen, C., Hunter, G., Gedeon, S., Eagar, T., 1987. Cinematography of resistance spot welding of galvanized steel. Weld. J. 66 (9), 2–60.

Liu, T., Wang, H., Yang, H., Ke, C., Zhou, L., Zhao, H., 2019. Microstructure of resistance spot weld ultra high strength steel Q&P980. IOP Conf. Ser. Mater. Sci. Eng. 612. doi:10.1088/1757-899X/612/3/032183.

Neid, H., 1984. The finite element modelling of the resistance spot welding process. Weld. J. 63 (4), 123–132.

Pouranvari, M., Alizadeh-sh, M., Marashi, S., 2015. Welding metallurgy of stainless-steel during resistance spot welding, part I: fusion zone. Sci. Technol. Weld. Join. 20 (6), 502–511.
Pouranvari, M., Marashi, S., 2012a. Failure mode transition in AISI 304 resistance spot welds. Weld. J. 91, 303–308.
Pouranvari, M., Ranjbarnoodeh, E., 2012. Dependence of the fracture mode on the welding variables in the resistance spot welding of ferrite-martensite DP980 advanced high-strength steel. Mater. Technol. 46 (6), 665–671.
Pouranvari, M., Marashi, S., 2010. Key factors influencing mechanical performance of dual phase steel resistance spot welds. Sci. Technol. Weld. Join. 15 (2), 149–155.
Pouranvari, M., Marashi, S., 2013. Critical review of automotive steels spot welding: process, structure and properties. Sci. Technol. Weld. Join. 18 (5), 361–403.
Pouranvari, M., Asgari, H., Mosavizadch, S., Marashi, P., Goodarzi, M., 2007. Effect of weld nugget size on overload failure mode of resistance spot welds. Sci. Technol. Weld. Join. 12 (3), 217–225.
Pouranvari, M., Marashi, S., 2012b. On failure mode of resistance spot welded DP980 advanced high strength steel. Can. Metall. Q. 51 (4), 447–455.
Shome, M., Tumuluru, M., 2015. Introduction to welding and joining of advanced high--strength steels (AHSS). In: Welding and Joining of Advanced High Strength Steels (AHSS). Woodhead Publishing, pp. 1–8.
Watanabe, G., Amago, T., Ishii, Y., Takao, H., Yasui, T., Fukumoto, M., 2016. Improvement of cross-tension strength using concave electrode in resistance spot welding of high-strength steel sheets. In: AIP Conference Proceedings doi:10.1063/1.4941202.
Zhang, H., Senkara, J., 2006. Resistance Welding: Fundamentals and Applications. Taylor & Francis, New York.
Zhou, K., Cai, L., 2014a. On the development of nugget growth model for resistance spot welding. J. Appl. Phys. 115 (16), 559–569.
Zhou, K., Cai, L., 2014b. Study on effect of electrode force on resistance spot welding process. J. Appl. Phys. 116 (8).